

GT2011-45- &

EXPERIMENTAL STUDY OF BLADE VIBRATION IN CENTRIFUGAL COMPRESSORS

Andrew H. Lerche
Southwest Research Institute®
San Antonio, Texas, USA

J. Jeffrey Moore, Ph.D.
Southwest Research Institute®
San Antonio, Texas, USA

Timothy C. Allison, Ph.D.
Southwest Research Institute®
San Antonio, Texas, USA

ABSTRACT

Blade vibration in turbomachinery is a common problem that can lead to blade failure by high cycle fatigue. Although much research has been performed on axial flow turbomachinery, little has been published for radial flow machines such as centrifugal compressors and radial inflow turbines. This work develops a test rig that measures the resonant vibration of centrifugal compressor blades. The blade vibrations are caused by the wakes coming from the inlet guide vanes. These vibrations are measured using blade mounted strain gauges during a rotating test. The total damping of the blade response from the rotating test is compared to the damping from the modal testing performed on the impeller. The mode shapes of the response and possible effects of mistuning are also discussed. The results show that mistuning can affect the phase cancellation which one would expect to see on a system with perfect cyclic symmetry.

INTRODUCTION

Vibration in turbomachinery blades can be caused by flutter or forced response. Flutter is an aeroelastic instability where the aerodynamic forces induced from blade vibration transfer energy into the structure, increasing the stresses with each cycle of vibration [1]. Flutter can occur in uniform flow fields and is difficult to stop once initiated.

Forced response vibration in turbomachinery blades is caused by unsteady forces acting on blades. When these forces excite the blade at their natural frequency a resonant vibration condition occurs. This resonant condition is marked by an increase in the vibratory amplitude. These forces vary

periodically in time and can be caused by aerodynamic conditions or mechanical events such as blade rubs [1]. Chiang and Kielb categorize the aerodynamic forcing functions in turbomachinery blades as inlet distortions, wake disturbances, and potential disturbances [2]. Total pressure disturbances include inlet distortions and wakes disturbances, while static pressure disturbances include potential disturbances. Inlet and wake disturbances always originate upstream, while potential disturbances can originate upstream or downstream. This work will examine an example of a wake disturbance from the rotor-stator blade interaction of a centrifugal compressor.

The purpose of this experimental work is to obtain dynamic strain data from the blades of a rotating centrifugal compressor. This data can then be used for validating fluid-structure interaction (FSI) models and other numerical methods or models that attempt to predict blade stresses on operating machinery.

Blade failures due to high cycle fatigue in turbomachinery are a common and costly problem. When a machine experiences a blade failure it often results into the shutdown of the operation that the machine is supporting. This down time results in a loss of production. Blade failures also can cause significant damage to other areas of a machine when a blade or section of a blade fails and travels downstream through the rest of the machine damaging other components in its path. Although dynamic strain data on axial machines is abundant, there is little data available in the public domain on radial flow machines such as centrifugal compressors and radial inflow turbines. The data from this experiment will provide some understanding to the structural response of centrifugal

compressor blades while in operation and experiencing resonant vibrations.

Recently, Kammerer and Abhari performed experimental studies on vibrating centrifugal compressor blades due to forced response [3]. Their test set up uses a closed loop single stage centrifugal compressor that simulates varying ambient pressures. They concluded that blade dynamics during resonance could be modeled with a single degree of freedom (SDOF) system if the overall critical damping ratio can be estimated. They then presented their approach to experimentally determine the critical damping ratio [4]. In addition to the experimental studies, Zemp, Kammerer, and Abhari investigated the inlet distortion of the centrifugal compressor using unsteady CFD [5]. This investigation was intended to quantify the forcing function acting on the blade surface due to inlet flow distortion. The above referenced works are important because they add to the very sparse experimental research for forced response vibrations in centrifugal compressors. The work presented below is unique in that the experiment relies on the wakes coming from the inlet guide vanes to excite the blade resonance, instead of inlet distortion screens. The work presented below also shows how mistuning effects can affect mode shapes and the occurrence of phase cancellation.

More recently, Lerche, Moore, and Feng [6], used the data from the rotating test, presented in this work, to compare to a coupled fluid-structure computational model. Their computational model correlated very well to the experimental data. The data presented below can also be used for the development of FSI modeling methods on centrifugal compressors.

EXPERIMENTAL TEST SETUP

The test rig is in an open loop configuration utilizing an un-shrouded (i.e. the shroud is not attached to the compressor but is attached to the stationary frame) centrifugal compressor and a vaneless diffuser. The shroud is made from a nylon material to prevent damage in a rub event. Air enters through the inlet consisting of fifteen (15) IGV's, flows through the compressor and is then discharged into an open plenum. Figure 1 shows a diagram of the test rig. The compressor is mounted using two sets of ball bearings, one on the drive end (DE) and the other on the non-drive end (NDE) of the compressor.

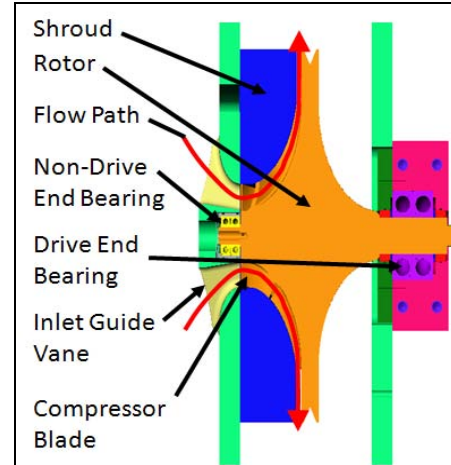


Figure 1. Cross section of test rig.

The test rig is powered by a 200 horsepower electric motor controlled by a variable frequency drive (VFD) and is connected to a eleven-to-one (11:1) speed increasing gearbox capable of driving the centrifugal compressor to 40,000 rpm (See Figure 2).

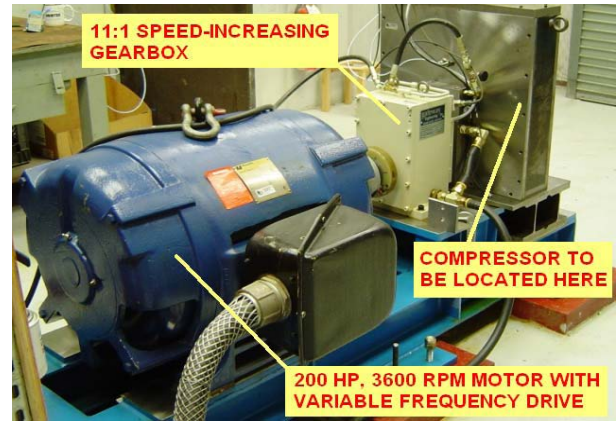


Figure 2. Experimental test rig with motor and gearbox.

Each time a compressor blade passes an inlet guide vane (IGV) it experiences an excitation caused by the wake from the IGV. In order for the blade to vibrate at resonance, the resonant frequency of the compressor blades must be known. Since there are fifteen (15) IGV's, a compressor blade will receive fifteen (15) excitations per a revolution. Thus the running speed necessary to excite the blade mode can be calculated by the following expression:

$$N_r = \frac{60\omega_n}{n_{igv}} \quad (1)$$

Where:

N_r is the speed of the compressor in rpm

ω_n is the blade natural frequency in Hz

n_{igv} is the number of inlet guide vanes

Although the blade resonance will increase slightly with speed, the non-rotating blade resonance will approximate where the test rig needs to run for the purposes of setting up and designing the test rig. For the compressor being tested, the increase in resonance frequency due to stress stiffening is approximately 1.5 percent when the compressor is rotated at 30,000 rpm.

Compressor

The rotor used in this experiment is a centrifugal compressor which was designed for research purposes. It was initially used in a novel centrifugal gas turbine design where the compressor and turbine sections were located integrally on one disc [7]. However, for this experiment only the compressor section is used, and the turbine section is machined off. The compressor is machined from 15-5ph stainless steel and is an open design, where the shroud is mounted on the stationary section of the test rig. The rotor contains twelve (12) main blades and twelve (12) splitter blades. The compressor is 11.81 inches in diameter. Figure 3 shows the centrifugal compressor that is used in the experiment.

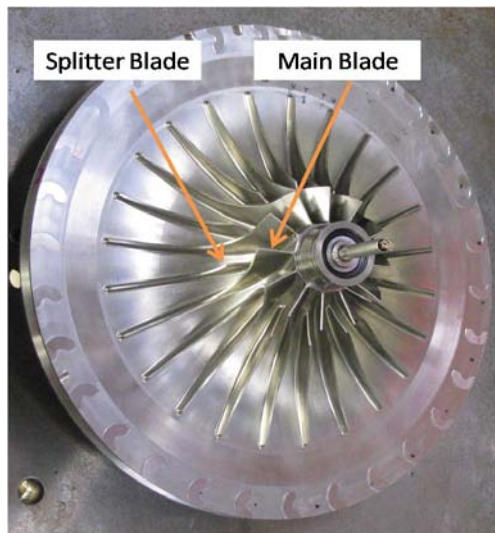


Figure 3. Centrifugal compressor used in test rig.

Strain Measurements

The compressor has two (2) of its twelve (12) blades instrumented with strain gauges. Each blade consists of a half-bridge strain gauge configuration where a strain gauge is mounted on each side of the blade, directly opposing each other. This configuration allows measurement of the bending stresses, so that strains due to centrifugal effects will not affect the measurement. In a half bridge configuration, the top and bottom side strain gauges should theoretically have the same magnitude of strain but just in opposite directions.

The strain gauges are mounted on the blade so that the direction of measurement is parallel with the leading edge of

the blade. The gauges are close to the leading edge of the blade near the blade root, where stresses are the largest. The wires to the strain gauges are then led through radial holes in the compressor and routed out an axial hole through the non-drive end of the compressor where they are connected to an amplifier. The signals from the amplifier are then passed to the data acquisition system by the use of a slip ring. A strain amplifier is necessary because the anticipated values of strain being measured are small and also because the signals are being passed through a slip ring, which introduces noise. Figure 4 below shows a strain gauge mounted on one of the compressor blades.

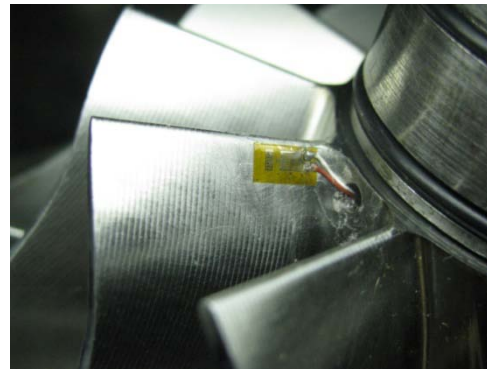


Figure 4. Photograph of strain gauge on suction side of one of the compressor blades.

Pressure and Temperature Measurements

In addition to strain measurements, pressure, temperature, and flow measurements are taken to monitor the performance of the compressor. Two total pressure probes are used at the compressor exit (adjacent to the outer diameter of the compressor). The probes are placed 180 degrees away from each other and two are used for redundancy. The total pressure probes are Kiel head type probes and are insensitive to yaw and pitch up to ± 45 degrees. At the compressor inlet, dynamic pressure is measured.

Total temperature at the compressor exit is measured using two half shielded thermocouples with an exposed junction. They are placed, like the total pressure probes, 180 degrees apart from each other. Since the test rig draws in ambient air, the ambient temperature and barometric pressure are measured.

Mass flow rate is measured by using an orifice plate in the exhaust pipe. The absolute pressure is measured on the upstream flange, and a differential pressure transducer is used to measure the pressure drop across the orifice, with taps at the flanges. Temperature measurements are taken from the upstream flange. Flow straighteners were used at the exhaust pipe entrance to promote uniform, swirl-free flow for more accurate orifice plate flow measurements. The mass flow rate is controlled by a valve downstream from the orifice plate.

Additional Instrumentation

An optical tachometer is used for speed and phase information, and it targets the compressor coupling. The tachometer is also used by the data acquisition system to track multiple orders. The data acquisition system used in this experiment is capable of tracking up to a 15X vibration, which is the same order of the blade vibration. A microphone is placed on the inlet plate of the test rig to confirm the excitation frequency, and also to monitor any other noise which may occur during testing. Figure 5 shows the front of the test rig with some of its instrumentation.

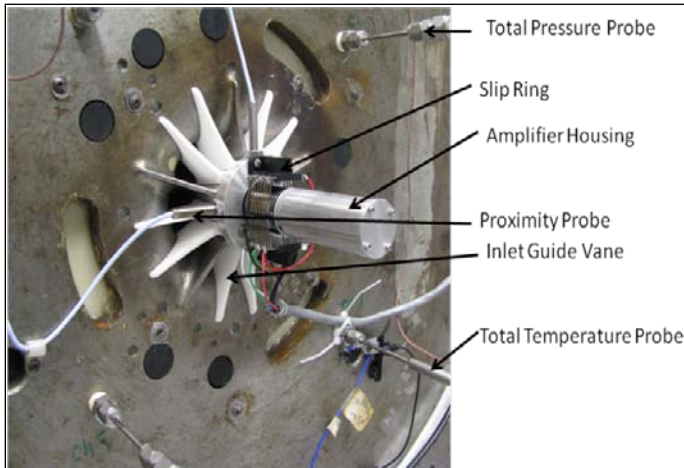


Figure 5. Photograph showing front of test rig.

MODAL TESTING

A modal test was performed on the compressor prior to the rotating strain test to determine the natural frequencies corresponding to blade dominated modes. This testing was performed by striking each blade tip of the un-mounted compressor with a modal hammer then recording its response with the strain gauges mounted on the compressor. Two (2) of the twelve (12) blades were instrumented for strain measurement. The two (2) blades are 180 degrees apart. The strain gauges are placed at the anticipated location where the dynamic strain is the highest on the blades. This occurs near the blade root and leading edge of the blade. The same strain gauges and amplifier are used in the rotating test. Modal testing plays an important role in tuning the models to match the actual compressor. The modal test helps to understand the dynamic behavior of the compressor and helps to predict approximately where the blade resonances will occur. The natural frequencies of the blade resonances will increase during the running test due to stress stiffening effects. Figure 6 shows the modal testing frequency response with six modes. A multi-degree of freedom, multi-FRF algorithm was used to determine the natural frequencies [8]. The mode shapes are shown in Figure 8 through Figure 13. The blade frequencies are needed so that the running speed at which the blade resonance occurs can be determined before running the test rig. With fifteen (15) IGV's

the compressor should experience the blade resonance around 17,600 rpm (4400 Hz).

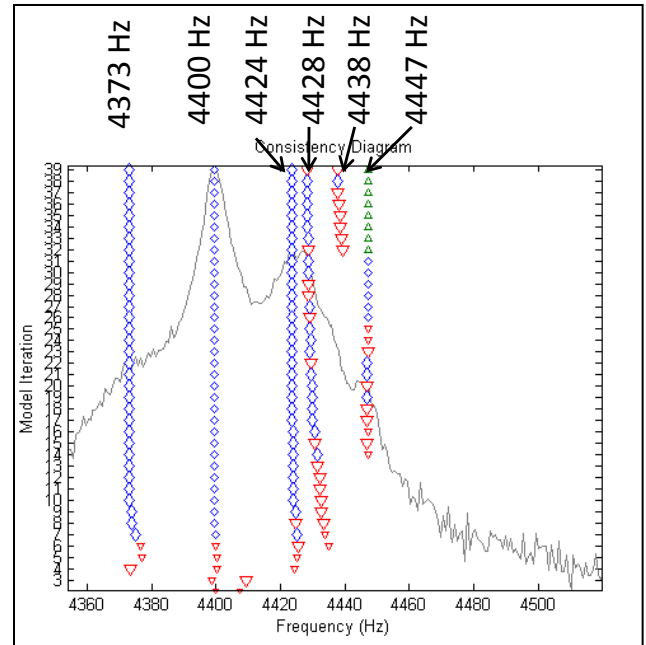


Figure 6. Frequency response of strain gauge on compressor blade.

MODAL ANALYSIS

A finite element analysis (FEA) model is built to compare against the modal test. The model here simulates the compressor in its un-mounted configuration. When the compressor is mounted in the test rig the frequencies will change slightly as it will be supported by bearings at each end. The resulting differences are explained later in the section.

The mesh used for the models consist of a mixture of tetrahedral and hexahedral elements. There are a total of 255,794 nodes and 76,787 elements. Most of the elements are approximately 0.25 inches and the two blades that are instrumented are refined with elements approximately 0.03 inches in size (See Figure 7). This mesh was developed for a FSI model where 360 degree mapping of pressures to the structure is required. Furthermore, the actual compressor has holes drilled adjacent to the two (2) instrumented blades to route the strain gauge wires. These holes, along with the strain gauges, introduce mistuning in the actual compressor. The mesh was tuned to match the mode shapes observed in modal testing, which revealed some asymmetry. For these reasons a cyclic symmetric model was not used.

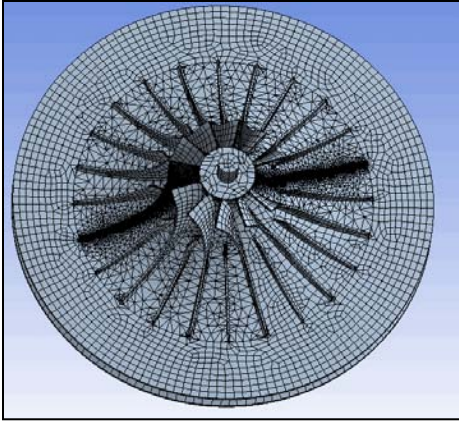


Figure 7. Mesh used in FE models.

The modal testing of the compressor revealed that the first blade mode is at 4,373 Hz, while the finite element analysis predicted the first blade mode at 4,398 Hz. This first blade mode appears to be a single nodal diameter mode and shows the two finely meshed blades out of phase with each other. Figure 8 through Figure 10 compare the finite element modal analysis to the experimental modal testing. The image on the right shows lines representing the blades. The black lines represent the displaced blade, while the red line represents the un-deformed blade. Nodal diameters are indicated by the dashed blue lines. This mode shape is also seen in the actual compressor. The modal testing determined the second mode to be at 4,400 Hz where the finite element modal analysis predicted the mode at 4,445 Hz (See Figure 9). This mode consists of two opposing blades responding in phase and in the same direction, while the remaining ten blades are also in phase but with less participation. This mode resembles a zero (0) nodal diameter mode since the blades are in phase. The third blade mode found by the experimental modal testing is at 4,424 Hz, while the finite element analysis showed the mode at 4,481 Hz (See Figure 10). This third mode consists of the two finely meshed blades moving in opposite directions from each other, while the remaining blades have some participation and respond in various directions. The nodal lines shown are not equally spaced circumferentially due to the asymmetry caused by the two (2) finely meshed blades. Figures 11-13 show additional modes measured at 4,428, 4,438, and 4,447 Hz. These modes are a result of blade mistuning and do not correspond as well to the modal analysis. The corresponding damping values for all the modes in the modal analysis are shown in Table 1. These damping values are determined using the polyreference time domain method for modal analysis.

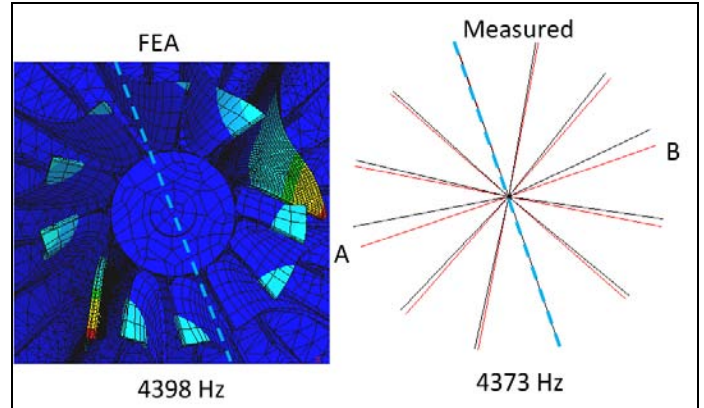


Figure 8. Comparison of first blade mode.

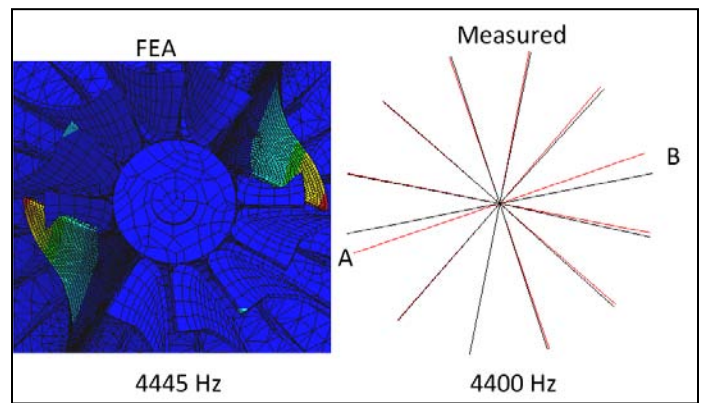


Figure 9. Comparison of second blade mode.

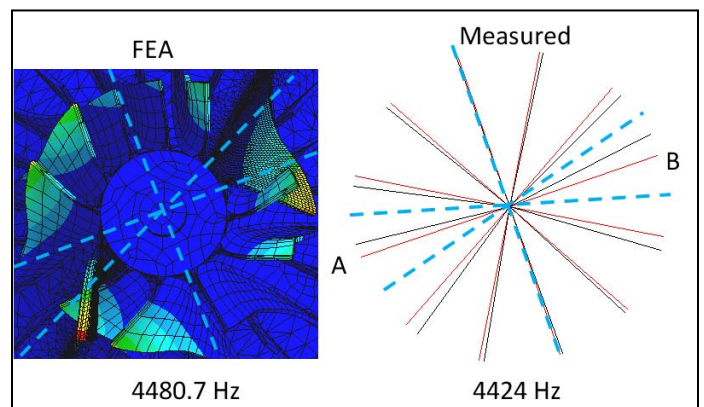


Figure 10. Comparison of third blade mode.

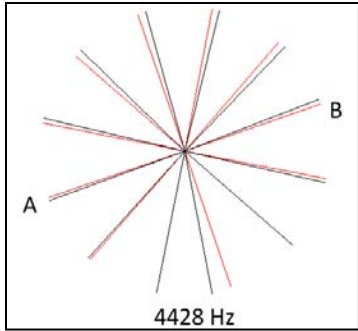


Figure 11. Measured blade mode at 4428 Hz.

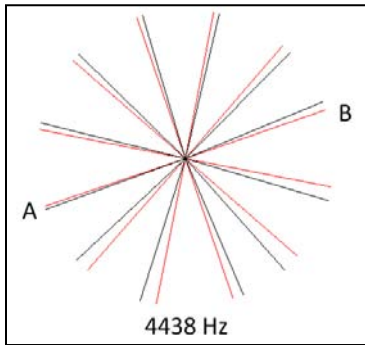


Figure 12. Measured blade mode at 4438 Hz.

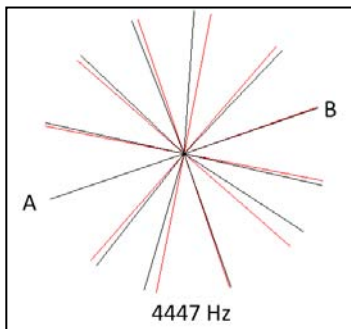


Figure 13. Measured blade mode at 4447 Hz.

Table 1. Experimental modal damping values.

Frequency	4373 Hz	4400 Hz	4424 Hz	4428 Hz	4438 Hz	4447 Hz
Modal Damping	0.339%	0.064%	0.138%	0.047%	0.036%	0.058%

Stress Stiffening Effects

A modal analysis is performed that considers stress stiffening effects caused by the centrifugal forces from rotation. This model will help determine where the blade response will occur and will also help to understand the mode shape of the response. This model includes centrifugal effects assuming 17,851 rpm and uses constraints at the bearing surfaces. The rotational speed of 17,851 rpm was determined by iterating several models until the resulting modal frequency matched the

rotational speed, assuming 15X excitation from the inlet guide vanes. Figure 14, Figure 15, and Figure 16 show the mode shape and frequency of the blade modes. The three frequencies are at, 4,462.8 Hz, 4,473.9 Hz, and 4,511.1 Hz.

The first mode shows two opposing blades in phase (0 nodal diameter mode), while the second mode shows two opposing blades out of phase (1 nodal diameter mode), and the third mode shows two sets of blades out of phase (2 nodal diameter mode).

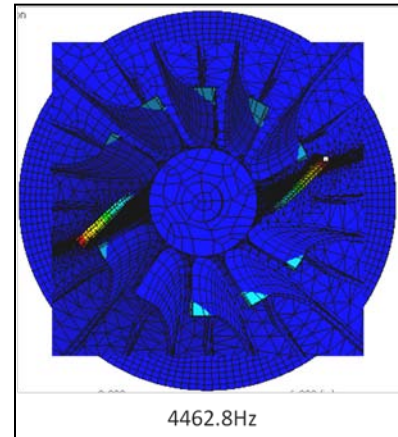


Figure 14. First blade mode with stress stiffening effects.

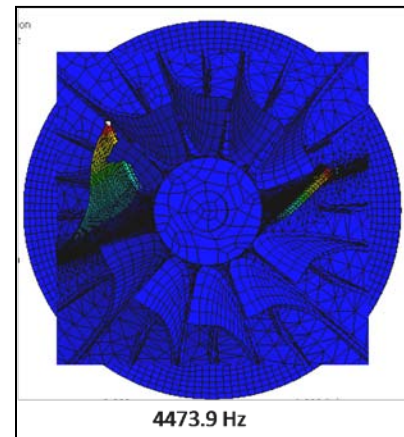


Figure 15. Second blade mode with stress stiffening effects.

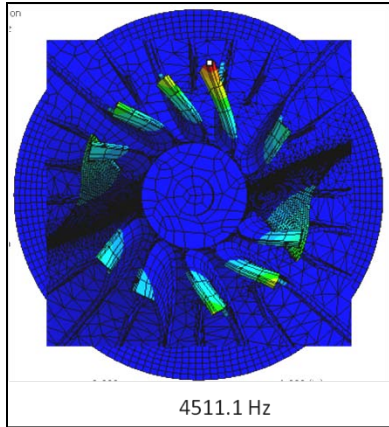


Figure 16. Third blade mode with stress stiffening effects.

These three modes differ from the FE modal analysis performed of the un-mounted compressor. The main differences are that stress stiffening effects were added, and constraints were added at the bearing locations. Without the stress stiffening effects, but with the bearing constraints, these first three modes change to 4435.8 Hz, 4446.2 Hz, and 4484.6 Hz. Since there is a difference in the un-mounted and mounted FEA modal analyses, the analysis with the mounted configuration should be compared to the rotating strain tests.

COMPRESSOR TESTING

The main purpose of the testing is to measure the dynamic blade strain due to blade vibration on a centrifugal compressor so that this data can then be compared to computational models that predict dynamic strains. The strain is measured all the way through the blade resonance, which occurs at approximately 4430 Hz. In addition to the structural response, performance data and mass flow rate are also obtained so that it can be used to compare to CFD models.

The testing procedure started by running the test rig through the blade resonance, to 19,500 rpm. The rig was kept running at 19,500 rpm until a steady state temperature was reached. Then three (3) speed sweeps were performed by ramping down slowly from 19,500 rpm to 15,000 rpm and slowly back up to 19,500 rpm. These speed sweeps captured the blades resonant response, which occurred around 17,700 rpm (4425 Hz).

Blade Strain Results

The strain response was monitored using a Bode plot which shows the response magnitude and phase versus the speed. In this case, the blade resonance is excited by the fifteen (15) inlet guide vanes, which means that the blades see fifteen (15) excitations in one revolution. When this excitation frequency is the same as the blade natural frequency it experiences resonant vibration. This resonant condition occurs approximately at 17,730 rpm (4430 Hz). Since the 15X (fifteen cycles per a revolution) response is of primary interest, a 15X band pass filter is used on the Bode plot so that no other

excitation orders are included in the response. Figure 17 and Figure 18 show the 15X response for blade A and blade B, respectively, for the nominal flow case (100 percent flow). A total of seven (7) speed sweeps are performed to demonstrate repeatability of the results.

Figure 17 shows the Blade A resonant response with a large peak at approximately 17,730 rpm (4,432.5 Hz), and a smaller peak at approximately 17,550 rpm (4,387.5 Hz). These two peaks represent two different modes. The peak response is 300 microstrain at 17,730 rpm (4,432.5 Hz). The smaller peak is 54 microstrain at 17,630 rpm (4,408 Hz).

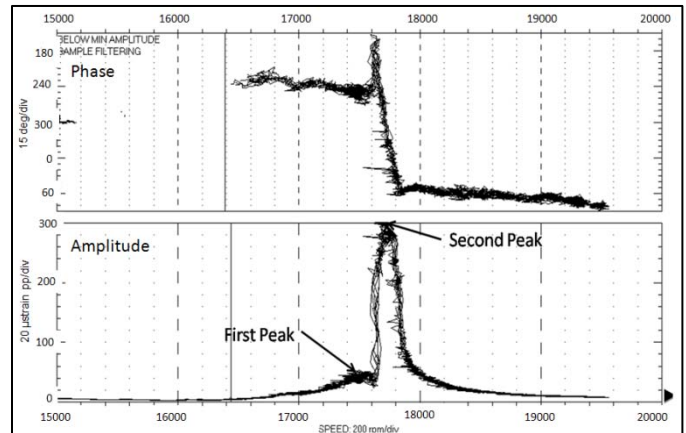


Figure 17. Bode plot showing strain response of blade A for nominal flow case.

Figure 18 shows the Blade B resonant response. There are three distinct peaks. The largest peak is 280 microstrain at 17,720 rpm (4,430 Hz). The smaller two peaks are 244 microstrain at 17,630 rpm (4,408 Hz), and 146 microstrain at 17,810 rpm (4,453 Hz).

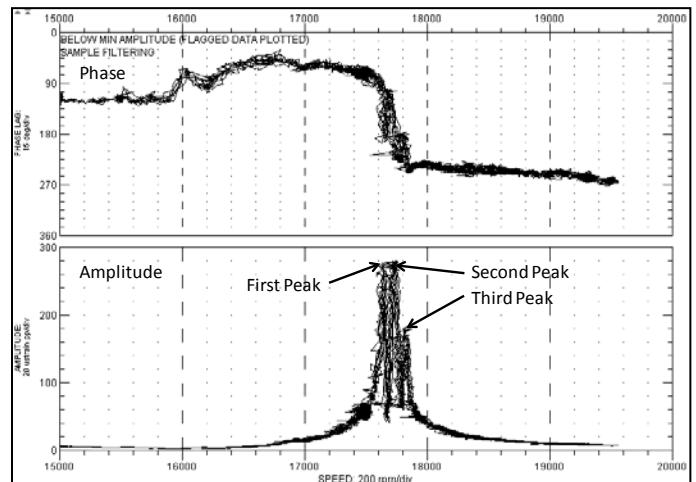


Figure 18. Bode plot showing strain response of blade B for nominal flow case.

The third peak that is seen in Blade B is more difficult to see in Blade A when looking at Figure 17. However, three

resonances can be seen in Blade A by looking at the Nyquist plot in Figure 19. Figure 20 shows a Nyquist plot for Blade B, and the three resonances are also clearly seen. These plots also show that the large modes near 17,730 rpm are out of phase. It can also be seen that the response amplitude of the first blade mode is much smaller in Blade A than in Blade B. This is likely due to manufacturing differences in the blades and strain gauge placement.

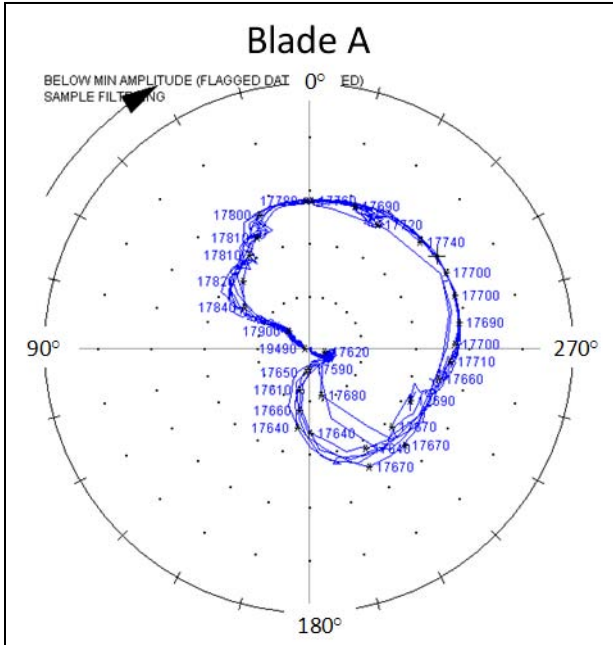


Figure 19. Nyquist plot showing blade A response.

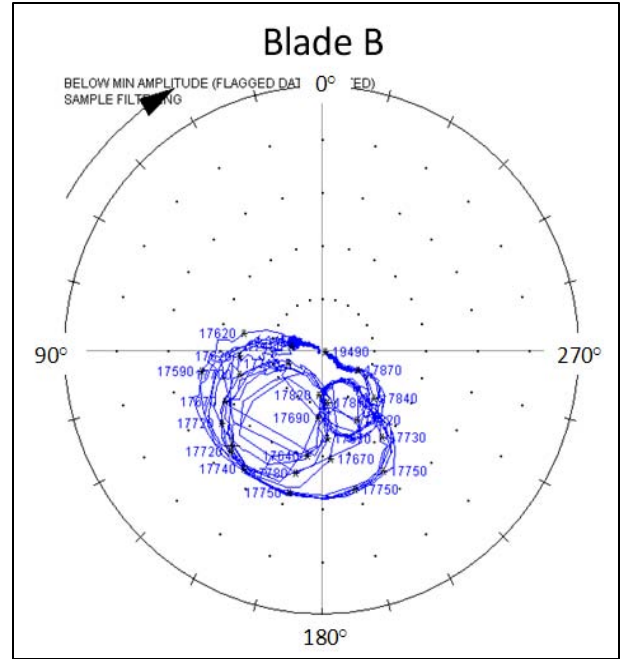


Figure 20. Nyquist plot showing blade B response.

Damping

The total damping of the blades consists primarily of material damping and aerodynamic damping. The material damping is internal to the material of the structure while aerodynamic damping is damping caused by the air surrounding the blades. The total damping is calculated by applying the half-power method to the experimental data. The half power method is given by the following equation:

$$\zeta = \frac{1}{2} \frac{f_2 - f_1}{f_n} \quad (2)$$

Where:

ζ is the damping ratio

f_1 and f_2 are the frequencies in hertz where the amplitudes of the response are $\frac{1}{\sqrt{2}} U_{\max}$

f_n is the resonant frequency in hertz

U_{\max} is the response amplitude at the natural frequency

The total damping, which includes material and aerodynamic damping, for the large peak of Blade A is 0.45 percent. Table 2 summarizes the experimental damping values for the blades A and B for the nominal flow case. Peak 2 shows that blades A and B are mostly out of phase. The damping calculated for blade A was used to simulate a single degree of freedom (SDOF) response, which is compared with the measured data in Figure 21. This shows that the damping determined from the half power method matches the data well. It must be noted that the half power method may not predict the

damping as accurately if there are other modes in close proximity or if half-power points are not present. For these cases other damping estimation methods may be used such as the circle fit method as described in Craig and Kurdila [9].

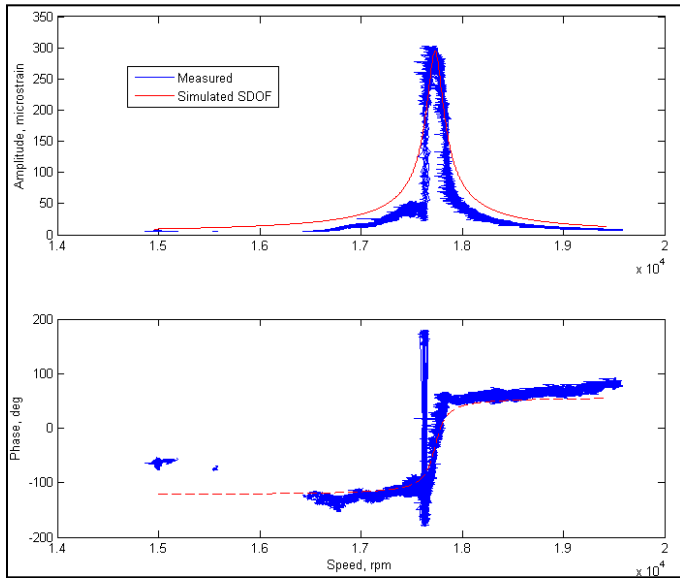


Figure 21. Simulated SDOF response using damping from half power method for blade A.

Table 2. Response data for blades A and B at resonance.

Nominal Flow Case		Peak 1		Peak 2		Peak 3	
	Units	Blade A	Blade B	Blade A	Blade B	Blade A	Blade B
Frequency	[Hz]	4,388	4,408	4,433	4,430	none	4,448
Speed	[rpm]	17,550	17,630	17,730	17,720	none	17,790
Amplitude	[microstrain]	54	244	300	280	none	146
Phase	[degrees]	255	133	315	174	none	208
Damping Ratio		0.0037	0.0011	0.0045	0.0043	none	0.0011

DISCUSSION

The stress stiffened modal analysis shows three distinct blade modes involving a zero (0) nodal diameter blade mode, a one (1) nodal diameter blade mode, and a two (2) nodal diameter blade mode. These are the only modes where the two finely meshed blades are active, and in these modes they are the blades with the most participation. The second peak on both instrumented blades occurs at approximately the same speed, and the blades respond out of phase indicating the mode to have an odd numbered nodal diameter. This mode is likely the one (1) nodal diameter mode that the stress stiffened modal analysis predicted to be at 4,473.9 Hz. The modal testing revealed that the three (3) nodal diameter blade mode is at 4,424 Hz. The models show that stress stiffening will increase the natural frequency by at least 1% for that mode shape when rotating at 17,851 rpm. This would place the frequency of the three nodal diameter mode, above any of the frequencies observed during testing, thus confirming that the one (1) nodal diameter mode is the largest peak.

This result shows that fifteen (15) IGV's and twelve (12) compressor blades can result in a one (1) nodal diameter mode. Kushner, Richard, and Strickland [10] discuss that when the difference in stationary blades and compressor blades is equal to the number of diameter nodal lines resonance will be largest, thus the compressor discussed here should show three (3) nodal lines. This deviation from the above nodal diameter rule shows that phase cancellation does not occur as it is expected, as in a symmetric system. This deviation is likely due to mistuning effects and also because the impeller in this research is unshrouded, so that the blades are not as closely coupled to the disc modes.

The results also show that there are elements of mistuning that effect the blade response. This mistuning comes from geometric conditions due to machining tolerances, strain gauges, and also from material differences in the compressor that create asymmetry. The holes drilled in the compressor that allow the strain gauge wires to pass through introduce mistuning since holes were drilled for only two of the blades. If all blades could be instrumented with strain gauges, all the blade modes could be identified, along with the participation of each blade in the different modes. However, this was not possible due to limitations with only having two channels available on the strain conditioner as well as limited channels to transmit the signal through the slip ring.

The strain data also shows the influence of aerodynamic damping. It was shown from modal testing that material damping is approximately 0.064 percent for the one nodal diameter mode. This value is the material damping as well as the damping from the surrounding air at atmospheric pressure. The rotating test shows that total damping (material damping and aerodynamic damping) was approximately 0.45 percent. This shows that aerodynamic damping is approximately 0.386 percent for the atmospheric inlet pressure tested here.

CONCLUSIONS

An experimental test rig was developed to measure the forced blade response of centrifugal compressor blades. The test successfully measured the blade resonance, capturing valuable information about damping and blade response. Modal testing was performed on the compressor blades to determine its natural frequencies corresponding to blade dominated modes and modal damping. This damping is small compared to the aerodynamic damping determined from the rotating test. A modal analysis was also performed of the impeller to help understand the compressor mode shapes. It was determined that the mode with the maximum response is likely a one-nodal diameter mode, which means it is possible to excite blade modes with n nodal diameters when the difference between the number of stationary vanes and rotating vanes is not equal to n . This also shows that phase cancellation in centrifugal compressors with mistuning present does not have the same

effect as it would with systems containing a high degree of cyclic symmetry.

REFERENCES

- [1] A. V. Srinivasan, "1997 IGTI Scholar Paper: Flutter and Resonant Vibration Characteristics of Engine Blades," *Journal of Engineering for Gas Turbines and Power*, vol. 119, October 1997.
- [2] H. D. Chiang, Kielb, R.E., "An Analysis System for Blade Forced Response," in *Transactions of the ASME*. vol. 115, 1993.
- [3] A. Kammerer, Abhari, R., "Experimental study on impeller blade vibration during resonance Part 1: Blade Vibration due to inlet flow distortion," in *Proceedings of ASME Turbo Expo 2008: Power for Land, Sea and Air GT 2008*, vol. GT2008-50466 Berlin, Germany, 2008.
- [4] A. Kammerer, Abhari, R., "Experimental Study on Impeller Blade Vibration During Resonance Part 2: Blade Damping," in *Proceedings of ASME Turbo Expo 2008: Power for Land, Sea and Air Berlin, Germany, 2008*.
- [5] A. Zemp, Kammerer, K., Abhari, R.S., "Unsteady CFD Investigation on Inlet Distortion in a Centrifugal Compressor," in *Proceedings of ASME Turbo Expo 2008: Power for Land, Sea and Air GT 2008*, Berlin, Germany, 2008.
- [6] A. Lerche, Moore, J.J., Feng, Y. "Computational Modeling and Validation Testing of Dynamic Blade Stresses in a Rotating Centrifugal Compressor Using a Time Domain Coupled Fluid-Structure Computational Model," in *Proceedings of ASME Turbo Expo 2010: Power for Land, Sea and Air GT 2010*. vol. GT2010-22216 Glasgow, UK, 2010.
- [7] K. Brun, McKee, R., Moore, J., Gernentz, R., Hollingsworth J., Smalley, A.J., "A Novel Centrifugal Flow Gas Turbine Design," in *Proceedings of the ASME Turbo Expo 2004: Power for Land, Sea and Air*, Vienna, Austria.
- [8] B. Peeters, Van Der Auweraer, H., Guillaume, P., Leuridan, J.; "The PolyMAX frequency-domain method: a new standard for modal parameter estimation", *Shock and Vibration*, 11 (2004) 395-409.
- [9] R.R. Craig, Kurdila, A.J., *Fundamentals of Structural Dynamics*, Second Edition, John Wiley & Sons, Hoboken, New Jersey, 2006.
- [10] F. Kushner, Richard, S.J., Strickland, R.A., "Critical Review of Compressor Impeller Vibration Parameters for Failure Prevention," in *Proceedings of the twenty-ninth Turbomachinery Symposium*, Houston, Texas, USA, 2000.